

University of Groningen

## Laser cooling, trapping and spectroscopy of calcium isotopes

Mollema, Albert Kornelis

**IMPORTANT NOTE: You are advised to consult the publisher's version (publisher's PDF) if you wish to cite from it. Please check the document version below.**

*Document Version*

Publisher's PDF, also known as Version of record

*Publication date:*

2008

[Link to publication in University of Groningen/UMCG research database](#)

*Citation for published version (APA):*

Mollema, A. K. (2008). *Laser cooling, trapping and spectroscopy of calcium isotopes*. s.n.

### Copyright

Other than for strictly personal use, it is not permitted to download or to forward/distribute the text or part of it without the consent of the author(s) and/or copyright holder(s), unless the work is under an open content license (like Creative Commons).

The publication may also be distributed here under the terms of Article 25fa of the Dutch Copyright Act, indicated by the "Taverne" license. More information can be found on the University of Groningen website: <https://www.rug.nl/library/open-access/self-archiving-pure/taverne-amendment>.

### Take-down policy

If you believe that this document breaches copyright please contact us providing details, and we will remove access to the work immediately and investigate your claim.

Downloaded from the University of Groningen/UMCG research database (Pure): <http://www.rug.nl/research/portal>. For technical reasons the number of authors shown on this cover page is limited to 10 maximum.

# Chapter 7

## Summary and outlook

### 7.1 Summary

The goal of the  $\text{Al}^{41}$ Catraz setup is to develop a laser cooling and trapping-based method to detect the abundance of  $^{41}\text{Ca}$  (which is in the order of  $10^{-15}$ ) in a natural sample of calcium. To achieve this goal, many facets of laser cooling and trapping of even and especially odd isotopes of calcium need to be known in great detail. In this thesis, aspects of laser cooling, trapping and laser spectroscopy on calcium isotopes are studied.

In Chapter 2 relevant elements of the structure of the calcium atom and the basics of laser cooling and trapping are introduced. In Chapter 3 the experimental setup is described. In Chapters 4, 5 and 6 data obtained with the  $\text{Al}^{41}$ Catraz setup between the summer of 2006 and the spring of 2008 are described and discussed.

In Chapter 4 a novel spectroscopy technique coined Light Pressure induced Spectroscopy (LiPS) is introduced and investigated. One of the most important features of the LiPS technique is that it produces a dispersivelike signal that can directly be used as an input for a laser frequency control loop, which makes the technique experimentally very simple and easy to apply. Experimental data are in good agreement with Monte Carlo simulations. The zero-crossing of the LiPS signal is approximately 0.1 - 0.2 line widths red-shifted from the atomic resonance frequency. The position of the zero-crossing depends only weakly on beam properties and laser power. The long term (several hours) frequency fluctuations when the laser was locked to the LiPS signal were measured to be 0.12 MHz only.

In Chapter 5 we have shown that with the current Zeeman slower enhancement ratios up to 500 can be reached. However, the actual velocity distributions of atoms leaving the Zeeman slower are not in agreement with the design goals of the Zeeman slower [20] nor with the simulations presented in Refs. [38, 85]. The position of the peak maximum appears to be somewhere between 60 – 100 m/s for all Zeeman slower parameters studied, while the design goal was to slow down the atoms to around 30 – 50 m/s. Simulations using the implemented design parameters predicted velocities

around 50 m/s as well. We can therefore conclude that not all the processes taking place in the Zeeman slower are well described in the simulations. The magnetic field of the Zeeman slower was measured. Comparison of the measured field with the theoretical optimum field shape reveals that the maximum initial velocity of the atoms that can be slowed down by the Zeeman slower is in the order of 470 m/s, which is well below the original design value of 1000 m/s.

In order to optimize the deflection stage, the MOT yield as a function of deflection laser power was measured. There appears to be a clear optimum at 11 mW. Decreasing MOT yield at higher powers is probably due to diffusive heating of the atomic beam. The gain in MOT yield resulting from compression of the atomic beam before the Zeeman slower is rather low. This might be due to the fact that the average interaction time of the laser beams with the atoms is rather short due to the high velocity of the atoms right after the oven (about 5 times shorter compared to the deflection stage) and/or to lateral heating during slowing of the beam in the Zeeman slower.

In Chapter 6 several aspects of the dynamics of Ca atoms trapped in a MOT are studied. The temperature of  $^{42}\text{Ca}$  and  $^{43}\text{Ca}$  atoms were measured and compared. The  $^1S_0 - ^1P_1$  transition in light even alkaline-earth isotopes like  $^{40,42}\text{Ca}$  and  $^{88}\text{Sr}$  forms an almost perfect two-level system. It is therefore an excellent testing ground for Doppler theory temperature predictions [44]. However, remarkably enough, the temperature of a cloud of trapped  $^{40}\text{Ca}$ , like all other even earth-alkaline isotopes trapped in a MOT so far, is higher than the temperature predicted by Doppler theory [16, 40, 43]. For odd isotopes of calcium, like  $^{43}\text{Ca}$  which possess hyperfine structure, one might instead expect a temperature well below the Doppler limit. Temperature measurements performed on an odd isotope of the earth alkaline Sr,  $^{87}\text{Sr}$  showed a clear sub-Doppler cooling effect [18].

The temperature of the MOT cloud of even Ca isotopes was measured using two methods, namely the release and recapture (RR) and cloud size method. Results from both methods turn out to be in good agreement with each other. The temperatures found are in good agreement with temperature measurements of  $^{40}\text{Ca}$  by others and are systematically far above the Doppler limit. Two recent models proposed to explain the temperatures of even alkaline earth isotopes in a MOT were tested. The model by Choi et al. (based on a density matrix approach) [51] was found to be fully consistent with the present data. The comparison with the model by Chanelière et al. (based on the influence of laser fluctuations on the temperature) [50] was less satisfactory.

The temperatures of even  $^{42}\text{Ca}$  and odd  $^{43}\text{Ca}$  isotopes were measured in identical circumstances using the RR method. No evidence was found for lower temperatures for the odd  $^{43}\text{Ca}$  isotope, which is in contrast with the results obtained from measurements performed on  $^{87}\text{Sr}$  by Xu et al. [18]. The absence of a sub-Doppler cooling mechanism in the case of  $^{43}\text{Ca}$  may be due to the level spacing and ordering of the hyperfine levels of the  $4s4p^1P_1$  state which differ from  $^{87}\text{Sr}$ . It seems that the exact hyperfine structure details inhibit significant sub-Doppler cooling.

Next, the trapping time of  $^{42}\text{Ca}$  in a MOT was measured for a wide range of trap settings. The results of the measurements can be understood using a rate equation model when an extra loss mechanism, the temperature dependent drift parameter, is

taken into account. Fitting the model to the data using this parameter yields temperatures which are in good agreement with actual temperature measurements performed for similar trapping conditions.

## 7.2 Outlook

As stated above, the goal of the Al<sup>41</sup>Catraz setup is to measure the level of <sup>41</sup>Ca in a natural sample of calcium. Key to the success of such a setup is the efficiency of the atom transport through the setup, i.e. the number of atoms that are trapped in the MOT with respect to the number of atoms evaporated from the oven. In his thesis, Hoekstra [20] estimates this efficiency to be in the order of  $10^{-6}$  and estimates an efficiency of  $10^{-2}$  to be feasible. However, a lot of experimental data is still needed to establish whether and how this efficiency can be achieved.

First of all, it is important to further investigate the characteristics of the atomic beam as it leaves the oven. The currently available data on the angular distribution and transversal velocity distribution as well as total flux is incomplete and inconclusive. Furthermore, several assumptions, like the assumption that the flow in the exit channels of the oven is laminar, have not been experimentally verified. Another issue is the total flux out of the oven. In order to complete an atom trap trace analysis (ATTA) measurement within a reasonable period of time, a relatively large amount of sample has to be processed. The flux can of course simply be increased by increasing the oven temperature. As a result of this, however, also the transversal velocity of the atoms will increase, which influences the efficiency of the setup.

Another part of the setup that should be investigated more thoroughly is the Zeeman slower. A large part of the data presented in Chapter 5 is well understood, but certain observations remain inexplicable. Besides that, the Monte Carlo simulations performed based on the Zeeman slower design parameters [38, 85] fail to correctly predict the velocity distribution presented in this thesis. Additionally, it turns out that the Al<sup>41</sup>Catraz Zeeman slower is unusually long. The longest Zeeman slower reported on in literature (besides ours) is about half as long as the one used in our setup [88] (cf. [47, 58, 91, 103]). A long Zeeman slower offers the opportunity to slow down a larger part of the original longitudinal velocity distribution of the atomic beam, however, it will also cause transversal heating, which results in an even more divergent beam. More over, if the atomic beam is not properly collimated at the time it enters the Zeeman slower, atoms will already be lost in the slower as a result of the initial divergence of the beam.

After the atoms leave the Zeeman slower they enter the deflection stage. In the current setup, the distance between the end of the Zeeman slower and the deflection stage is  $\sim 25$  cm. This distance can result in a reasonable amount of beam loss due to divergence of the beam. Another aspect of the deflection that could not be studied in the current setup is the optimal detuning of the deflection laser beam. Presently, the deflection laser beam has the same frequency as the MOT laser beams, so the frequency of the laser beams for both sections of the setup could only be tuned simultaneously.

Furthermore, a compression section right after the Zeeman slower should be considered to get the atoms in the beam on-axis, in order to increase the total flux towards the MOT.

Hitherto, there is no evidence that applying the ATTA scheme to  $^{41}\text{Ca}$  for abundances as low as  $10^{-15}$  is physically not feasible. It should nevertheless also be clear that it will still take quite some effort before such an ATTA measurement can be performed. In particular the transport efficiencies and throughputs for the different isotopes need further research.

### 7.2.1 A MOT fluorescence detection scheme for future ATTA measurements

During a successful ATTA measurement the abundance of  $^{41}\text{Ca}$  will be measured relative to another isotope of Ca, e.g.  $^{43}\text{Ca}$ , which possesses similar hyperfine structure. Given the fact that there is a difference in abundance of many orders of magnitude between the two isotopes that have to be measured, there will be orders of magnitude between the amount of MOT fluorescence to be detected during the two measurements. Such a wide range of fluorescence intensities cannot be covered by one and the same detector: a detector (in our case a PMT) configured to be sensitive enough to detect the fluorescence emitted by one single atom in the MOT (see [20]) will get completely over-exposed when it has to measure the fluorescence produced by a cloud of  $10^3 - 10^5$  trapped atoms. In the past, schemes using two different types of detectors have been proposed [104], using e.g. a CCD camera for the most abundant isotope and a PMT for the least abundant isotope. The difficulty of such a scheme lies in the calibration of these two detectors, given the fact that they are of a totally different type. A simple yet effective scheme to solve this issue is proposed here.

As explained in Chapter 3, over-exposure of the PMT as a result of large numbers of atoms in the MOT can be avoided by using a suitable neutral density filter (NDF). On the other hand, such a NDF should of course not be used if one tries to measure the fluorescence produced by one single atom trapped in a MOT. A simple setup to perform an ATTA measurement would therefore consist of two (preferably identical) PMTs both pointed at the MOT center. One of them should be shielded with a suitable NDF in order to measure the fluorescence of the isotope with highest abundance. By measuring the fluorescence of a very low number of atoms without a NDF mounted on either one of the PMTs both detectors can easily be calibrated with respect to each other.

### 7.2.2 Measuring isotope shifts with a CCD using laser induced fluorescence

The isotope shifts of the  $4s^1S_0 - 4p^1P_1$  transition in Ca has subsequently been measured by Brandt et al. [105], Andl et al. [106] and Nörtershäuser et al. [39]. The resulting data is presented in Fig. 7.1. Given the fluctuation in the data and the uncertainties, it

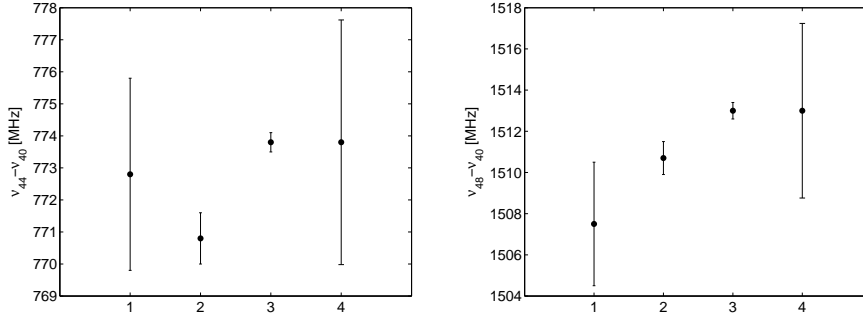


**Figure 7.1:** Different measurements of the  $4s^1S_0 - 4p^1P_1$  isotope shift for  $^{44}\text{Ca}$  (left) and  $^{48}\text{Ca}$  (right). 1:Ref. [105], 2:Ref. [106], 3:Ref. [39] and 4:Ref. [39] including a systematic error of 80 kHz/amu.

might be interesting to obtain a new set of data points for at least the natural isotopes with higher precision and accuracy.

A method is proposed to measure the isotope shift using induced fluorescence detected using a CCD. A schematic of the proposed setup is given in Fig. 7.2. A laser will be stabilized on the  $4s^1S_0 - 4p^1P_1$  transition in  $^{40}\text{Ca}$ . A weak probe beam is split off from the laser beam and sent through an AOM and a tunable EOM. This way, the probe frequency can be scanned over all the isotopes of interest. If the weak probe beam is in resonance with the atoms, the atoms will emit photons. This results in a fluorescence distribution in the atomic beam which can be measured using a CCD camera. Exactly like in Chapter 4, a cross section of the CCD image can be taken and the obtained fluorescence profile can be fitted with a Lorentzian line shape, from which the location of the peak can be determined, see Fig. 4.6(b). When the frequency of the laser shifts, the peak position will shift as well, so by taking several CCD images of the weak probe beam fluorescence, the peak position can be calibrated as a function of frequency change, as shown in Fig. 4.7. This data can be fitted with a straight line. Scanning the laser over a wide frequency range, such that the fluorescence of several isotopes of Ca can be detected, one will obtain a data set as shown in Fig.7.3. From the linear fit of the data of the different isotopes the frequency shift between the adjacent available isotopes can be found (see the arrows in Fig. 7.3). The accuracy will be determined by the absolute frequency stabilization as a function of time (measured to be 0.14 MHz [67] and the uncertainty from the Lorentzian fit.

Major advantage of this method compared to the older methods is that the frequency differences between the isotopes is directly measured. In contrast to older methods, the exact locking point of the laser is not important, as long as it stays constant during the measurements. Same goes for the exact pointing of the probe beam. Any (residual) Doppler shift will give rise to an overall shift of the absolute frequency

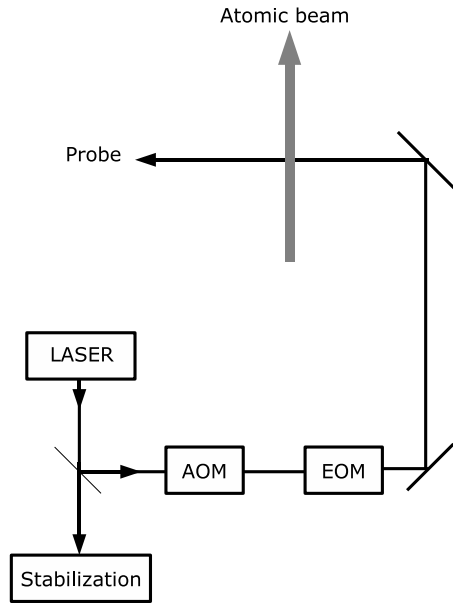
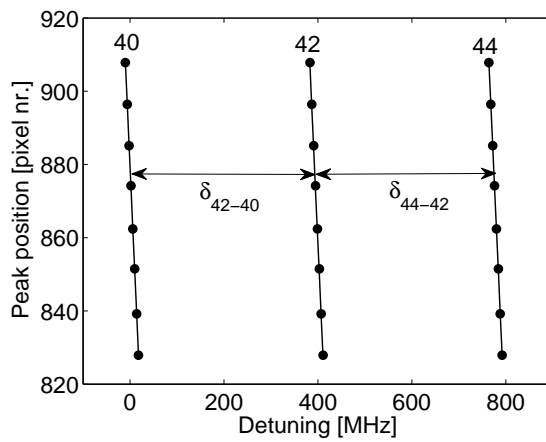


Figure 7.2: Schematic drawing of the proposed experimental setup.

at which the fluorescence is measured but will not influence the measured frequency difference between the isotopes.



**Figure 7.3:** Data that might be obtained using the proposed method. Solid lines are fits through the data. The actual isotope shift can be obtained from these fitted lines as indicated by the arrows.



